Int J Earth Sci (Geol Rundsch) (2002) 91:712–721
DOI 10.1007/s00531-001-0242-y

ORIGINAL PAPER

**Nico-Alexander Urbanski · Malte Vöge
Ralf Seyfried · Lars Rüpke · Tanja Petersen
Till Hanebuth · Matthias Hort**

Fifteen days of continuous activity survey at Stromboli volcano, Italy, in late September 2000: Doppler radar, seismicity, infrared, soil humidity, and mapping of the crater region

Received: 19 February 2001 / Accepted: 23 November 2001 / Published online: 22 January 2002

Abstract The intention of our study was to gain new insight into the complex interplay between different types of eruption of the Stromboli volcano by combining detailed field observation with different geophysical methods. We recorded more than 600 eruptions by use of continuous Doppler radar measurements. We detected the onset of the seismic precursor and the beginning of the visible eruption by use of seismic and infrared data. Two soil samples per day were used to monitor the effect of humidity on the eruptive style. We mapped the crater region as a reference base for the long-term morphological changes of the active region and for the exact positions of our measurement systems. Two distinct types of eruption were distinguished from each other on the basis of seismic and radar data – short, wide-angle Strombolian explosions and pulsating, sharp angle fountain-like eruptions. Data and visual observations imply that weather conditions significantly effect volcanic activity. We also interpret the intensification of eruptive activity during our field study as replenishment of the reservoir with a new batch of magma in late September 2000.

Keywords Stromboli volcano · Eruptive style · Weather influence · Monitoring · Doppler radar

N.-A. Urbanski (✉) · T. Hanebuth · M. Hort
Graduiertenkolleg "Dynamics of global cycles",
Wischhofstr. 1–3, 24148 Kiel, Germany
e-mail: nurbansk@geomar.de

M. Vöge · R. Seyfried · L. Rüpke · M. Hort
GEOMAR Forschungszentrum, Wischhofstr. 1–3,
24148 Kiel, Germany

T. Petersen
Institut für Geowissenschaften, Christian-Albrechts-Universität,
Olshausenstr. 40, 24118 Kiel, Germany

Introduction

Stromboli is the northernmost island of the Aeolian archipelago. The 924 m high island is the subaerial part of a large volcanic edifice rising from a depth of approximately 2,000 m b.s.l. in the Tyrrhenian Sea. The island has been built-up during the last 100,000 years (Gillot and Keller 1993). Seven main active periods were distinguished from each other on the basis of age determinations and lava composition (Hornig-Kjarsgaard et al. 1993). Rocks which erupted during different periods are easily distinguished from each other by their Sr^{87}/Sr^{89}-ratios and K_2O concentration varying from calc-alkaline, high-K calc-alkaline, shoshonitic to potassic in composition. During the two most recent periods (Neo-Stromboli), changes in chemical composition coincided with major flank collapses affecting the uppermost part of the volcanic edifice (Francalanci et al. 1989).

The last collapse event occurred approximately 5,000 years ago (Gillot and Keller 1993), forming the horseshoe-shaped Sciara del Fuoco (Fig. 1) and marking the onset of persistent activity. Typical activity of Stromboli is characterized by short, so-called Strombolian, gas-driven explosions and brief periodic pulsating lava fountains, interspersed with rare lava outflows and paroxysmal eruptions. There are historic reports of continuous activity since at least Greek times (ca. 4,000 years B.P.; Barberi et al. 1993) and an average of six to seven explosions per hour have been reported by Ripepe (1996). A very good presentation of the long term seismic activity can be obtained from Stromboli on-line (Carniel and Alean 2000).

The activity at Stromboli is restricted to the crater terrace at the upper end of the Sciara del Fuoco. Three active vents were located within this terrace during our field study in September 2000 (Fig. 2). On the basis of thermal modelling Giberti et al. (1992) suggested that only a shallow magma reservoir with continuous replenishment of magma batches enables this type of steady

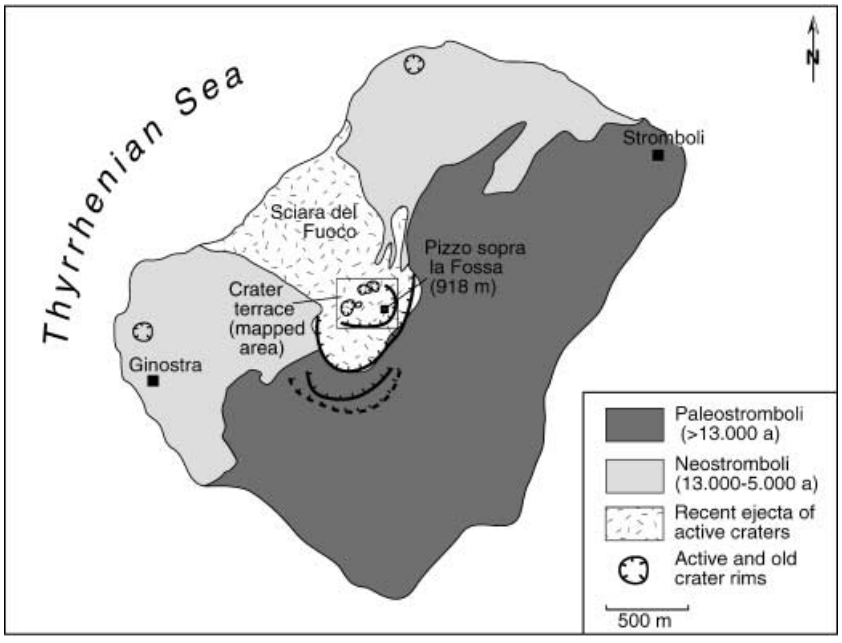

Fig. 1 Simplified geological overview of Stromboli island (after Hornig-Kjarsgaard et al. 1993). The *rectangle* marks, approximately, the mapped area of the crater terrace

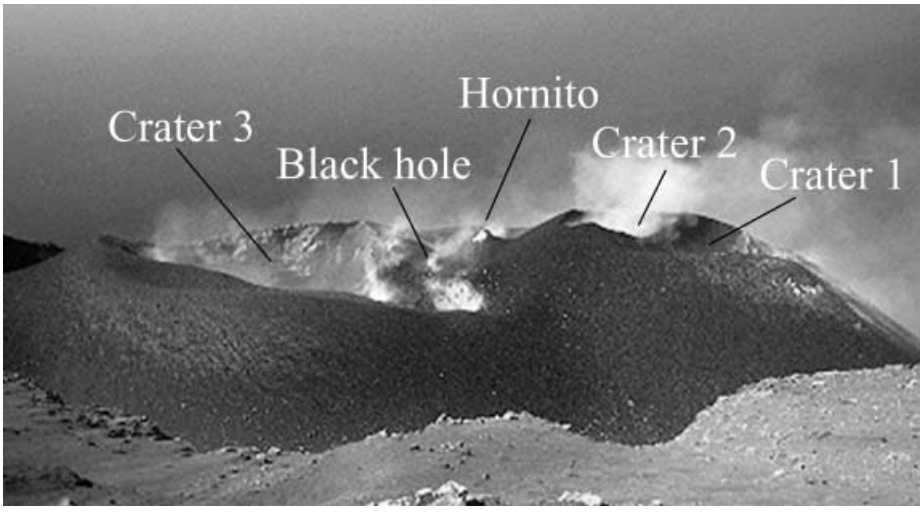

Fig. 2 Aerial photograph of the crater terrace, taken from the Pizzo sopra la Fossa looking to NW over the three active vents and other features described in the text and table

state activity. Although the source depth of the volcanic explosions and their tremor could be inferred from seismic data (Wassermann 1997) the reservoir geometry is still difficult to delineate from seismic data (Neuberg et al. 1994; Kirchdörfer 1999). Chouet et al. (1974) inferred the depth of the magma reservoir on the basis of eruption velocities. They measured the lengths of trajectories of incandescent particles on photographs recorded at 10 frames/s. Ripepe et al. (1993) improved this technique using film with maximum sensitivity in the near-infrared, and digital image analysis of successive frames. These photographic techniques have the disadvantage that all ejected particles that are either too small to be resolved on the film, or are no longer incandescent, will be suppressed in the record. Weill et al. (1992) used sonic Doppler measurements to infer that particles in the sub-cm-range make up the majority of the erupted material. These studies lacked continuous monitoring over several days and, as this study shows, single eruptive events are not representative of long-term eruption behavior. On the basis of sound measurements Vergniolle and Brandeis (1994) and Vergniolle et al. (1996) suggested that explosive eruptions were triggered by collapsing bubbles. Ripepe (1996) distinguished at least two different eruptive mechanisms for the explosions by combining sound and seismic measurements.

Here, we present the results of a 15-day-period of continuous survey of the three active craters of Stromboli in late September 2000 (13 to 27 September 2000, Julian day 256–270). Unlike former surveys we used Doppler radar for continuous monitoring of the eruptions and the associated particle velocities. As we will show, it is useful to distinguish between different types of eruption at Stromboli volcano. This, with seismic and infra-

red data, enables monitoring of a combination of seismic activity and eruption dynamics. Soil samples yielded data about the humidity of the volcano surface and thus some monitoring of the possible impact of the weather on the eruptive behavior. Crater mapping was performed to build a base for a long-term survey of the structural changes of the crater terrace. All data obtained were used in combination with visual observations of the activity to enable determination of the effect of weather on the eruptive style of Stromboli volcano. That the weather affects activity at Stromboli has been suggested by Neuberg (2000), on the basis of seismic evidence.

Observational techniques

Mapping of the crater area

We used a light-weight, compact Leica Vector GIS binocular. It uses a laser beam to measure distances and a magnetic compass to determine the declination and inclination without having to mark different target points. The theoretical precision of the distance measurements is approximately ±1 m within a measurement region of 1 m up to 1,000 m. The maximum angle error is ±1°. We made multiple reference measurements to estimate the actual mapping error.

Doppler radar

We employ a Doppler radar technique to overcome problems, e.g. eruption velocity (Hort and Seyfried 1998), associated with quantitative observations of eruption dynamics. A schematic drawing of the Doppler principle is shown in Fig. 3. For details on how the radar technique is implemented in our instrument (METEK MVR-3) the reader is referred to Klugmann et al. (1996) and Seyfried and Hort (1999). In its current design the entire system

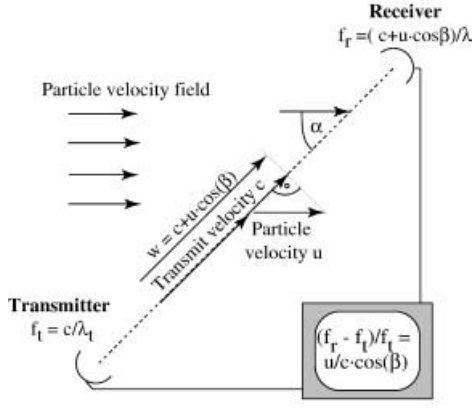

Fig. 3 Schematic drawing of the frequency shift of the Doppler effect. The transmit velocity c is superimposed by the component of the particle velocity field in the beam, direction w. The superposition of c and w generates beat f_r–f_t, the so-called Doppler shift

weighs approximately 20 kg, including all accessory equipment (except batteries) and can be transported in two backpacks. It consists of a transmitter and receiver unit, a separate box for signal processing, and a standard satellite dish for simultaneous focusing of beam and back-scattered signal with an aperture of 3°. The transmitted power of 50 mW with a 60 cm reflector is sufficient for measurements at distances less than 1 km. The output of the MVR-3 is the velocity distribution for 16 distance intervals of variable length (20–200 m), the so-called range gates. This data set is called the velocity–power spectrum; it can be read off the instrument via an RS 232 interface at intervals as short as 1 s.

DCF time synchronization is used for later correlation of the radar data with other measurement techniques recorded simultaneously (e.g. infrasound or seismic).

Data are recorded on a data-logger built around a low power-consumption PC 104 embedded computer board. It is equipped with a 6 Gb hard disk, which enables continuous data storage for approximately 7 days. The implemented software enables easy configuration of all measurement conditions, e.g. sampling rate, the range-gate length, or range-gate set-up. Start-up time of a measurement can be specified and the total reflected power is calculated automatically for each spectrum. When the reflected power reaches a specified threshold, the built-in trigger port activates a camcorder to record eruptions visually.

Seismicity and infrared monitoring

Seismicity was recorded by use of a one-component, vertical Lennartz seismometer (LE-1d/v-lite) with a flat frequency response from 1–80 Hz. Data were collected by means of a Psion data-logger at a sampling rate of 100 Hz simultaneously with the infrared signal. For this we used a conventional infrared diode mounted at the focus of a sampling lens; both were fixed in a stable aluminum tube on the logger case. The data-logger was operated in a triggered mode, enabling storage of each event 20 s before the trigger occurred and 40 s after the trigger, which was set to ±40 mV seismometer output, matching a ground velocity of 10^{-4} m/s.

Soil humidity

Soil sampling was performed to enable qualitative monitoring of the effect of humidity on the eruptive style of the volcano. Soil samples were taken halfway down the northern flank of the ridge south of the crater terrace (Fig. 4). The sampling location was shifted daily by approximately 40 cm to the east and samples were taken daily until 24 September 2000 except on 13 and 14 September 2000. The two rows of sample locations were approximately 4 m apart. The location was chosen because of its proximity to the craters and was retained to minimize local atmospheric effects (e.g. insolation) on soil

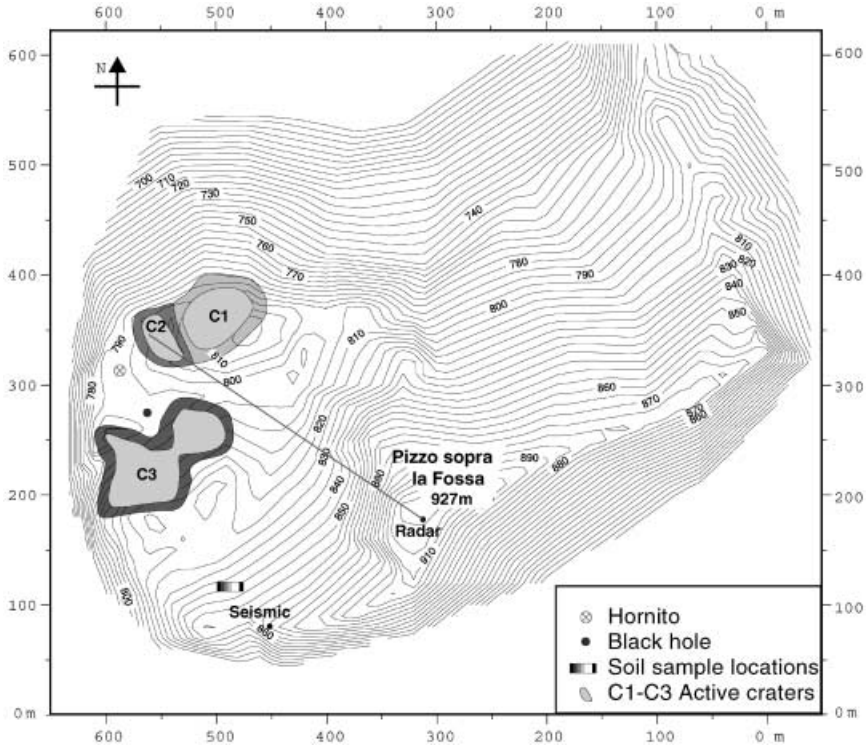

Fig. 4 Map of the crater terrace of Stromboli volcano obtained from Vector GIS binocular measurements. Marked are the three active craters (C1–C3), the positions of the seismometer, with the infrared sensor (seismic), and that of the radar instrument and the direction of the radar beam. The map also shows the area where the soil samples were taken

humidity. Two samples were taken per day, one in each row. Sampling was performed by digging a hole approximately 20 cm deep into the unconsolidated ground. A sampling flask was then pressed into the soft ash and sealed after removal to avoid water loss by diffusion and evaporation; it was later weighed before and after drying in an oven to determine the water content.

Results

Field observations

The daily observations of all active craters, visible degassing sites, and weather observations are summarized in Table 1. The overall activity of the vents increased from the beginning of the monitoring period with a peak during 20–26 September 2000 (J. day 263–269). On the last day of observation (27 September, J. day 270), the overall activity was extraordinarily low, compared with the previous 14 days. Activity changes and eruptive style are described for each active crater.

Crater 1, least active during the entire field study, was characterized by few ash plumes and laterally directed eruptions (approximately every 40 to 60 min), with scoria deposition approximately NNW down the Sciara del Fuoco.

Crater 2 was characterized by abundant explosions, in part laterally deflected towards crater 3 during the first three days (13–15 September 2000). Later, the eruptive style gradually changed to short, gas-driven Strombolian fountains (16, 17 September 2000). From 18–23 September 2000, culminating on the 20th, scoria was steadily thrown over and on to the crater rim. This activity ceased after 24 September 2000. Eruptions at crater 2 occurred every 15–30 min on average during our period of observation, except on 27 September 2000.

Crater 3 was nearly inactive at the beginning of the field study (13–17 September, J. day 256–260), except for minor gas eruptions, with convective ash plumes rising above the crater and minor pulsating lava fountains that hardly reached the crater rim. Similar behavior had previously been observed at this crater during 05/2000, after a heavy thunderstorm. The activity increased steadily culminating between 23 and 26 September (J. day 266–269), with frequent pulsating fountains.

Mapping of the crater region

Previous maps based on visual impressions (e.g. Harris et al. 1996; Carniel and Alean 2000) provided a very good overview of the main topographic features of the Stromboli summit region. These two-dimensional sketches give a good impression of the morphology but do not enable exact determination of distances or altitudes; this is necessary when trying to locate instruments. We therefore created our own topographic map (Fig. 4), using the technique described above, to locate our instruments and provide a base for future studies aimed at representing morphological changes of the active region.

Our map, based on 160 individual measurements, uses a geodetic point at the Pizzo sopra la Fossa as a fixed

Table 1 Summary of the activity of Stromboli volcano (*n.o.* no observations)

Date	Crater 1	Crater 2	Crater 3	Other craters/ Hornito	Degassing	Weather/ view	Comments	Soil samples
13.09.2000	One pulsating fountain observed from the ferry	Lateral and vertical Strombolian explosions	n.o.	n.o.	Strong degassing and vapour development	Rainfall 3 days before arrival	Soil is wet at surface	A taken at noon
14.09.2000	Ash plumes	Lateral Strombolian explosions	Several ash plumes, with ash-fall on Pizzo, few scoria erupted inside the crater (audible)	Rhythmic, noisy degassing	Strong degassing and vapour development	No wind, good view		B taken at noon
15.09.2000	Ash plumes	±Vertical Strombolian explosions and gas eruptions	Large, rising, and long-lasting ash plumes, with ash-fall on Pizzo, few scoria inside the crater	Noisy degassing, decreasing in the afternoon	Strong degassing and vapour development, decreasing in the afternoon	No wind, good view	Overall activity decrease in the afternoon	C/D taken at noon
16.09.2000	n.o.	Few vertical Strombolian explosions and pulsating fountains	Noisy degassing, no ash plumes observed; low, long-lasting, pulsating fountains	Noisy degassing, once scoria erupted from small crater and black hole	Strong degassing and vapour development before noon, vapour content decreases in the afternoon	No wind, good view		E/F taken in the afternoon
17.09.2000	n.o.	Pulsating fountains (every 15 min)	Few ash plumes and noisy degassing	Quiet degassing and few noisy degassing events at black hole	Strong degassing with no vapour	No wind, good view		G/H taken in the afternoon
18.09.2000	n.o.	Pulsating fountains (every 15–20 min), scoria thrown steadily over the crater rim	Sequences (every 30–45 min) of multiple, long lasting and (~30 s) high pulsating fountains (~80 m), no ash plumes	Quiet degassing	Strong degassing with no vapour	No wind, good view	Simultaneous eruptions from crater 2 and 3	I/J taken in the afternoon
19.09.2000	n.o.	Pulsating fountains (every 15–20 min), steady glowing	Sequences (every 30–45 min) of multiple, long-lasting and (~30 s) high pulsating fountains (~80 m) and ash plumes	Quiet degassing	Strong degassing with no vapour	Sirocco, good view	Simultaneous eruptions of crater 2 and 3	K/L taken in the afternoon
20.09.2000	n.o.	Scoria thrown steadily over the crater rim (up to 30 m high) and glowing, noisy degassing and bursting bubbles in the crater	n.o.	Quiet degassing	Low degassing, with no vapour	Sirocco, good view		M/N taken in the afternoon

Table 1 (continued)

Date	Crater 1	Crater 2	Crater 3	Other craters/ Hornito	Degassing	Weather/ view	Comments	Soil samples
21.09.2000	n.o.	n.o.	n.o.	n.o.	Strong, vapour rich degassing in the evening	Summit in clouds		No sample taken
22.09.2000	n.o.	Few observable, pulsating eruptions	n.o.	n.o.	Strong degassing with vapour development	Strong wind, bad view on the crater terrace		O/P taken in the afternoon
23.09.2000	Ash plumes (every 30–60 min)	Large pulsating fountains (every 20–30 min), scoria thrown steadily over the crater rim and noisy degassing	Long-lasting, ash-rich pulsating fountains (every 5–30 min)	Quiet degassing	Strong degassing, without vapour development, yellowish gas plumes	Good view		Q/R taken in the afternoon
24.09.2000	Ash plumes (every 20–40 min)	Large pulsating fountains (every 15–30 min), noisy degassing	Long-lasting, ash-rich pulsating fountains (every 5–30 min)	Quiet degassing	Low degassing and no vapour development	Good view		S/T taken in the afternoon
25.09.2000	n.o.	Large pulsating fountains (every 15–30 min), noisy degassing	Long lasting, ash-rich pulsating fountains (every 5–30 min)	Quiet degassing	Low degassing and no vapour development	Good view		No sample taken
26.09.2000	Few pulsating fountains	Few, low pulsating fountains (every 30 min)	Long lasting and high (>200 m) pulsating fountains (every 5–30 min), several pulses per eruption	Quiet degassing	Low degassing and no vapour development	Good view		No sample taken
27.09.2000	n.o.	Very few eruptions (every 60 min)	n.o.	Quiet degassing	Low degassing and no vapour development	Good view	Overall activity extremely low	No sample taken

reference point. Because the entire crater region was not visible from the summit, we used three reference points semi-encircling the active crater region from NE, E, and S. Positions were determined by repeated measurements from the Pizzo sopra la Fossa.

The general morphology of the Stromboli summit region is visualized using 5-m contour lines. The circular shape of the ridges and the inclined and domed surfaces around and in-between the walls of each crater are well portrayed.

Radar observation, seismicity, and infrared

More than 600 eruptions were recorded by use of Doppler radar during the field study. The visually observed differences in eruption style between the first and the last days of the field study are also reflected in both seismic and radar data (Figs. 5 and 6). Two examples are discussed here in more detail. Fig. 7a shows the velocity spectrum of the first 5 s of a pulsating fountain erupting from crater 3 on 27 September 2000 and Fig. 7b the velocity spectrum of the first 5 s of an explosion erupting

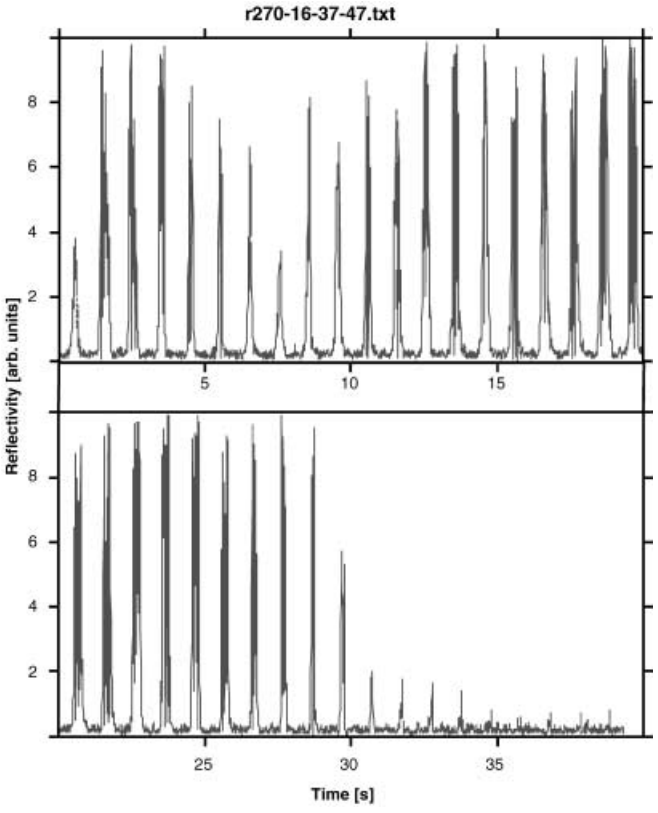

Fig. 5 Successive radar power spectra of a pulsating lava fountain. The MVR-3 transmits and receives simultaneously at 24 GHz. This signal is on-line low-pass filtered and FFT transformed. Plotted are the successive power spectra (time resolution 1 s) of all detected Doppler frequencies in the distance interval above the eruption herd. For each of the 16 distance intervals the detected Doppler frequencies are on-line digitized in 128 frequency steps. These Doppler frequencies are directly proportional to the velocities of the measured clasts. The amount of power displayed for each frequency step represents the reflected radar power from all targets moving with the related velocity. Hence, this power is a qualitative indicator of the mass moving with the related velocity. Each second one of these power spectra is recorded and displayed in this figure

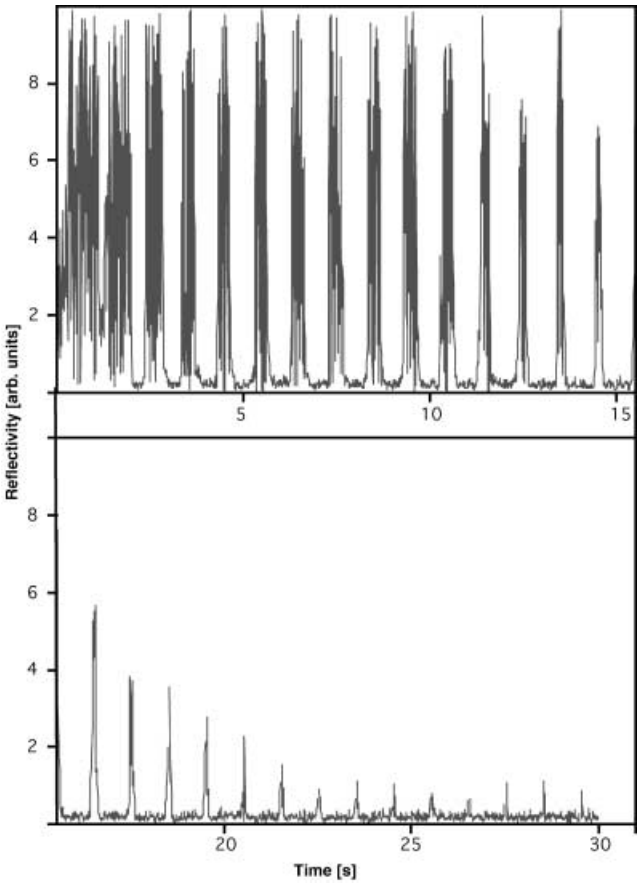

Fig. 6 Radar power spectra of a Strombolian explosion recorded and displayed in the same way as described in Fig. 5

from crater 2 on 18 September (J. day 261). Although the duration (~30 s) and maximum reflected energy of both events are of the same order of magnitude, their signal structures are quite different.

Pulsating fountains start slowly with a narrow low-velocity peak, their amplitude increasing and decreasing rhythmically (Fig. 7a). Peak reflectivity and, therefore, the highest density of pyroclasts in the fountain can be observed after the first half of the eruption. The eruption then decreases in a manner similar to its start. The radar signal remains in a narrow band over the entire time, also during the phase of back-falling pyroclasts. A narrow bandwidth of fall velocities indicates a small range of particle sizes, assuming that they settle at their terminal settling velocity.

Explosions (Fig. 7b) start with a broadband energy-rich signal, because of the wide solid angle distribution at which the particles were ejected from the center of the explosion. With time, the reflected energy of particles with positive velocities (rising particles) decreases quickly, indicating that the main mass of pyroclasts is expelled during the initial explosion. In addition, the solid angle at which particles are ejected becomes narrower as the conduit geometry exerts more control on the eruption process. The total reflectivity power decreases with time until the eruption ends.

The particle-size distribution of explosions is much more difficult to extract from the radar signal. The wide solid angle at which particles pass through the radar beam produces a wide range of projections of these velocities on the radar beam, making it impossible to distinguish between velocity and angle. Here, three-dimensional measurements are necessary for clear definition of the complete velocity vector. We performed some of these measurements during our field study but their evaluation is beyond the scope of this paper.

The seismic signals associated with both types of eruption are shown in Fig. 8, which depicts the features of the radar observations. The pulsating fountain of crater 3 (Fig. 8a) starts smoothly, almost without a precursor, with the signal remaining at a relatively low value until it is overlain by strong transients of ground-colliding clasts. The bursts at the end of this seismic event

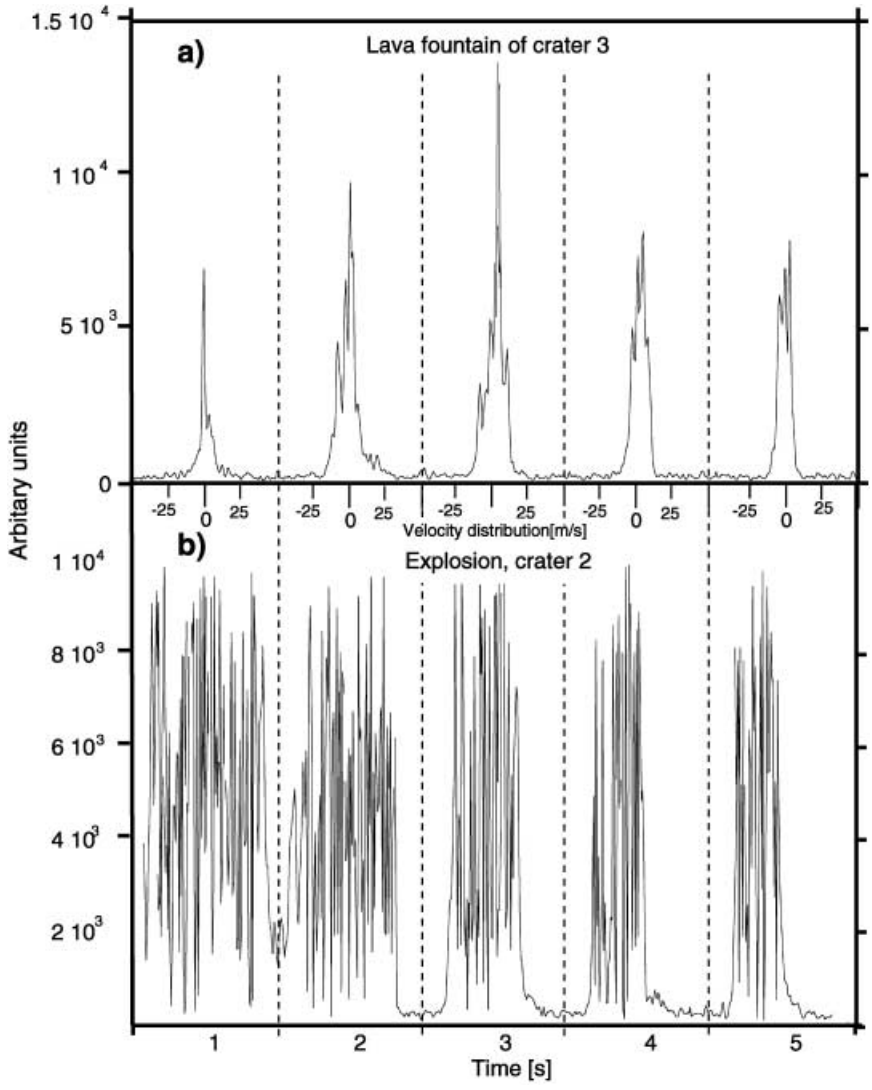

Fig. 7a, b Comparison of the first five Radar spectra of both detected eruption types. **a** The pulsating fountain from Fig. 5; **b** the Strombolian explosion of Fig. 6. Each spectrum shows the measured velocity power spectrum component projected into the vertical from –50 to 50 m/s

probably originate from the rhythmic pulsations of the eruption fountain. The seismic signal of an explosion at crater 2 (Fig. 8b) shows a clear precursor of 8 s. The following very steep transient reflects the air wave reaching the seismometer 1 s after the onset of the eruption as detected by the infrared diode. The first transients of the ground-colliding particles are observed only a few seconds later.

There is a clear difference between the amplitudes of the ground-colliding particles of both events. The seismometer was placed approximately 180 m from crater 3 (pulsating fountain) and particles reached the ground at distances less than 100 m from the seismometer. Thus, their signal is much stronger than those of the back-falling particles at crater 2, at a distance of approximately 280 m (distances obtained from the map; Fig. 4). Another possible explanation of differences between the amplitudes of signals from the back-falling particles is the range of particle sizes, being produced by either eruption type and thus determined by the different fragmentation processes in the conduit. The composition of the ground, and slight differences between this, might also alter the signal originating from back-falling particles.

The number of seismic events per day for the entire field study (Fig. 9) have a clear peak in the period of the observed activity increase of the volcano after the September 20 which ends sharply with the end of our measurements on September 27.

Soil humidity

During an earlier study, in May 2000, a shift in magmatic activity towards more explosive behavior was observed after a heavy thunderstorm passed over the island. Daily soil samples were taken during this field study to enable detection of the effect of humidity. Their water content decreased systematically with time (Fig. 10), consistent with the increasing aridity of the soil after rainfall 3 days before we began our measurements.

This coincides with the already described decrease in the abundance of explosions during the first 3 days of

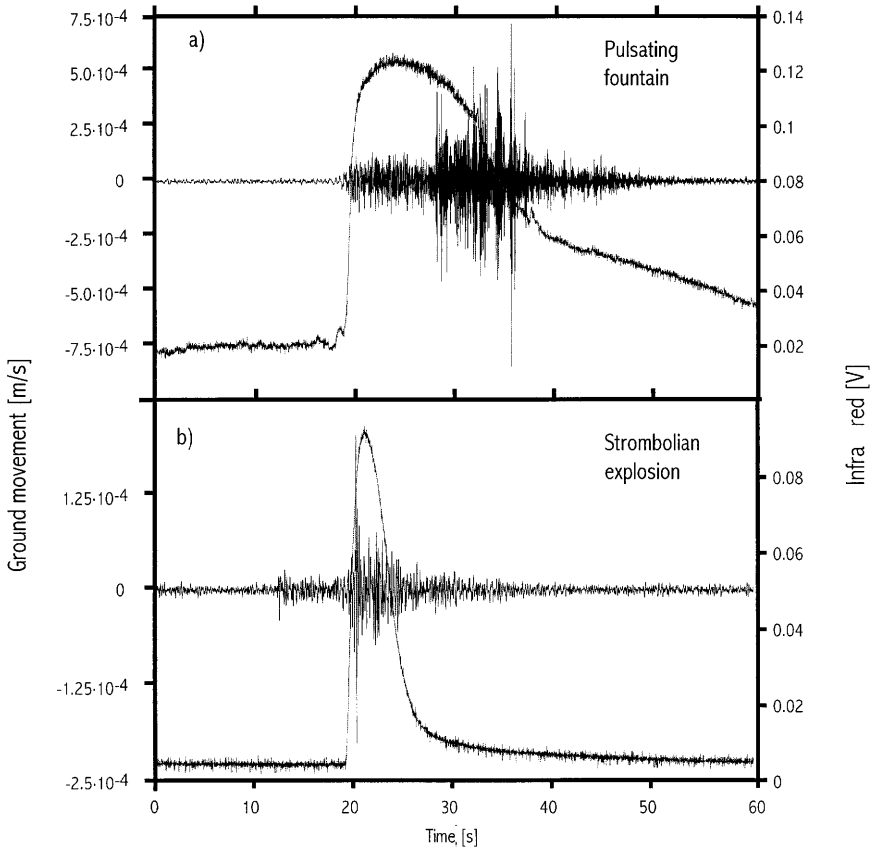

Fig. 8a, b Examples of the seismicity of the two types of eruption depicted in Fig. 7. **a** Pulsating fountain; **b** Strombolian explosion. The steep transients in the second half of the signals are a result of ground-colliding particles

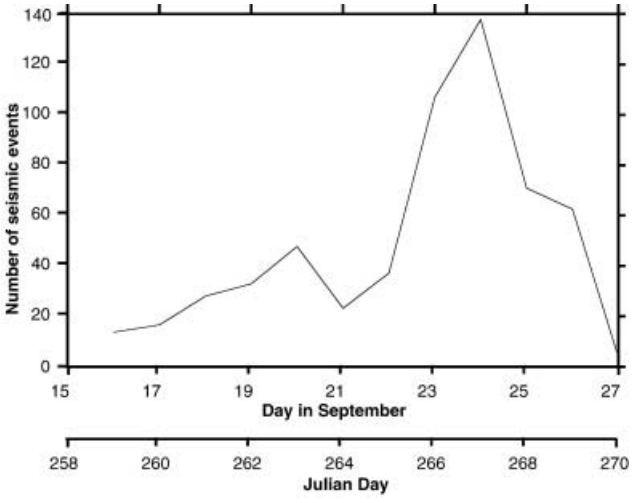

Fig. 9 Number of seismic events per day plotted against the days. The plot shows a clear peak from 23 to 26 September simultaneous with the increasing activity of crater 3

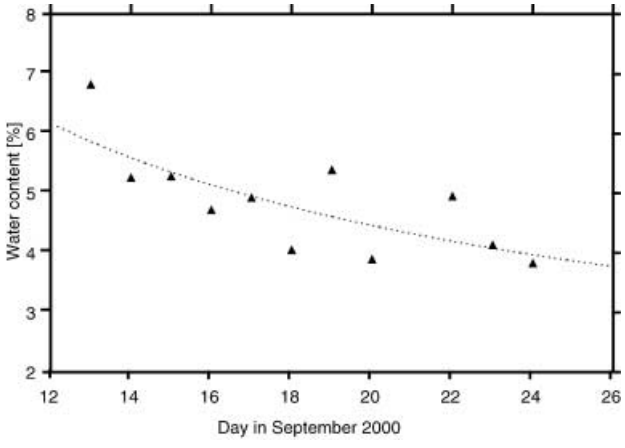

Fig. 10 Water content of soil samples taken on Stromboli between 14 and 24 September 2000. Except for the first 2 days the data points represent an average from two samples

our observations. We hasten to emphasize that these results are only a first glimpse on the inferred connection between weather and the activity of Stromboli and should, therefore, be treated with caution.

Conclusions and outlook

The increasing unrest of the volcano and the observation of steady scoria throwout of crater 2 during at least 5 days (20–25 September 2000) suggest a rising magma level in the conduit. This suggestion is supported by the observation of the free surface magma level inside crater

2, which, together with the increasing activity of crater 3 (from 23 September, J. day 266 on), indicates that a fresh batch of magma might have reached the low level magma reservoir of Stromboli. Seismic data provide further evidence of elevated activity from 23 to 27 September 2000.

We obtained two distinct seismic signal patterns in accordance with Ripepe (1996), strongly related to mass movement fluctuations during the eruptive phase. Analog experiments of Seyfried and Freundt (2000) suggest that Strombolian explosions are caused by bursting of one single bubble. These bubbles (so-called slugs) can reach tens of meters in length, because of their hydrostatic decompression. Seyfried and Freund (2000) also found that slugs can reach ascent velocities greater than 10 m/s for Strombolian conditions (2 m conduit diameter, 100 Pa s magma viscosity) if they remain connected to their source (supplied slugs). The disruption of a supplied slug at the surface leads to a short explosion with a wide angle aperture of the expelled clasts.

Pulsating fountains, in contrast, originate from slug flow and the observed pulsations are produced by the sequential bursting of single bubbles. Slug flow forms because of degassing at depth, its frequency content being more complex. Resonance frequencies of single bubbles are superimposed with the resonance of the entire bubble-magma column (with widely unknown geometry).

The effect of weather ranges from altering the morphology of the craters to cooling of the entire edifice, including the uppermost parts of the magmatic system. We observed an obvious change in eruptive style and overall activity with decreasing humidity.

The activity at crater 2 was dominated by noisy explosions during the first three days, successively shifting to pulsating fountains. We thus assume that the eruptive style at Stromboli is strongly influenced by weather, as a result of water–magma interaction during humid periods. Unconsolidated ash and scoria is washed into the craters during rainfall, blocking the narrow conduit of crater 3. This explains the quiescence of crater 3 after rainy periods. Gas accumulates below the blockage and the conduit is successively cleared by gas outbursts, forming convectively rising ash plumes. Pulsating fountains develop again when these obstacles are removed from the conduit exit. In addition, blocking of crater 3 might increase the lava level in crater 2, which was obviously reset as a result of the increasing activity of crater 3. This observed interplay between both craters suggests that they are supplied by one shallow magma reservoir, consistent with the seismic analysis of Neuberg et al. (1994).

Acknowledgements Thanks are extended to Pierre Cottens for lending us his generator, without which this study would not have been possible, to Dannielle Pestalozzi for her patience with our noise while testing our broken gasoline generator, and to H.-U. Schmincke for improving the manuscript. Financial support by the Deutsche Forschungsgemeinschaft (HO 1411/10–1) to M. Hort and the Graduiertenkolleg “Dynamik globaler Kreisläufe” (grant SCHM 250/49) to H.-U. Schmincke and financial support by the state of Schleswig–Holstein is gratefully acknowledged.

References

Barberi F, Rosi M, Sodi A (1993) Volcanic hazard assessment at Stromboli based on historical data. Acta Vulcanol 3:173–187

Carniel R, Alean J (2000) Stromboli on-line http://stromboli.net

Chouet B, Hamisevicz N, McGetchin TR (1974) Photoballistics of volcanic jet activity at Stromboli, Italy. J Geophys Res 79:4961–4976

Francalanci L, Manetti P, Peccerillo A (1989) Volcanological and magmatological evolution of Stromboli volcano (Aeolian Islands): the roles of fractional crystallization, magma mixing, crustal contamination and source heterogeneity. Bull Volcanol 51:355–378

Giberti G, Jaupart C, Sartoris G (1992) Steady-state operation of Stromboli volcano, Italy: constraints on the feeding system. Bull Volcanol 54:535–541

Gillot PY, Keller J (1993) Radiochronological dating of Stromboli. Acta Vulcanol 3:69–77

Harris AJL, Stevens NF, Maciejewski, AJH (1996) Thermal evidence for linked vents at Stromboli. Acta Vulcanol 8:57–61

Hornig-Kjarsgaard I, Keller J, Koberski U, Stadlbauer E, Francalanci L, Lenhart R (1993) Geology, stratigraphy and volcanological evolution of the island of Stromboli, Aeolian arc, Italy. Acta Vulcanol 3:21–68

Hort M, Seyfried R (1998) Volcanic eruption velocities measured with a micro radar. Geophys Res Lett 25:13–16

Kirchdoerfer M (1999) Analysis and quasistatic FE modeling of long period impulsive events associated with explosions at Stromboli volcano (Italy). Ann Geofis 42:379–390

Klugmann D, Heinsohn K, Kirtzel HJ (1996) A low cost 24 GHz FM CW Doppler radar rain profiler. Beitr Phys Atmos 69: 247–253

Neuberg J, Luckett R, Ripepe M, Braun T (1994) Highlights from a seismic broadband array on Stromboli volcano. Geophys Res Lett 21:749–752

Neuberg J (2000) External modulation of volcanic activity. Geophys J Int 162:232–240

Ripepe M, Rosi M, Saccorotti G (1993) Image processing of explosive activity at Stromboli. J Volcanol Geotherm Res 54: 335–351

Ripepe M (1996) Evidence for gas influence on volcanic seismic signals recorded at Stromboli. J Volcanol Geotherm Res 70: 221–233

Seyfried R, Hort M (1999) Continuous monitoring of eruption dynamics: a review of various techniques and new results from a frequency modulated radar Doppler system. Bull Volcanol 60:627–639

Seyfried R, Freundt A (2000) Analog experiments on conduit flow, eruption behavior, and tremor of basaltic volcanic eruptions, J Geophys Res 105:23727–23740

Vergniolle S, Brandeis G (1994) Origin of sound generated by Strombolian explosions. Geophys Res Lett 21:1959–1962

Vergniolle S, Brandeis G, Mareschal, J-C (1996) Strombolian explosions 2. Eruption dynamics determined from acoustic measurements. J Geophys Res 101:20449–20466

Wassermann J (1997) Locating the sources of volcanic explosions and volcanic tremor at Stromboli volcano (Italy) using beamforming on diffraction hyperboloids. Phys Earth Planet Int 104:271–281

Weill A, Brandeis G, Vergniolle S, Baudin F, Bilbille J, Fevre JB, Piron B, Hill X (1992) Acoustic sounder measurements of the vertical velocity of volcanic jets at Stromboli volcano. Geophys Res Lett 19:2357–2360